Note on mirror birefringence in a Fabry-Perot cavity

Yuta Michimura[1, 2, *]

[1] *LIGO Laboratory, California Institute of Technology, Pasadena, California 91125, USA*
[2] *Research Center for the Early Universe (RESCEU), Graduate School of Science, University of Tokyo, Tokyo 113-0033, Japan*

(Dated: August 24, 2022)

This note describes some of basic effects of mirror substrate and coating birefringence in a single Fabry-Perot cavity. Here we mainly consider uniform static birefringence. Higher-order modes are not considered until the last section. This document is LIGO-T2200272.

I. SUMMARY

- When ITM fast axis and ETM fast axis are aligned or orthogonal to each other, polarization eigenmodes of the cavity will be linear, and mode-matching will be maximized when the input polarization is aligned to either axis. Polarization rotation will not happen in this case.
- Alignment requirement for such case will not be severe, i.e. within a few degrees or so, since the effect is quadratic to rotation angles.
- Requirements on roll motion of mirrors or input beam polarization rotation for future gravitational wave detectors with AlGaAs coating will be in the order of $1\times(1\ \mathrm{Hz}/f^2)\ \mathrm{nrad}/\sqrt{\mathrm{Hz}}$, even in the worst case scenario when ITM and ETM axes are rotated 45 degrees to input polarization. When axes are aligned, the requirement will be significantly relaxed.
- Phase of the orthogonal polarization generated in the reflection of cavity is always $\pi/2$ off from the phase of input beam, if birefringence is small enough.
- For ITM substrate birefringence, the amount of TEM00 mode in unwanted polarization stays the same when the cavity is unlocked or locked. The amount of higher order modes will be reduced after lock, from Lawrence effect.
- For ETM coating birefringence, the amount of TEM00 mode in unwanted polarization increases when the cavity is locked. The Lawrence effect will not work completely for higer order modes.
- When there is enough uniform static birefringence that resonant frequencies of two polarization eigenmodes split more than a cavity linewidth, effects will be even further relaxed, as orthogonal polarization will be off-resonant.

The effects from power and signal recycling cavities and unbalanced BS reflectivity/transmission for unwanted polarization needs to be studied further. Axis symmetric coating noises can be calculated in a usual way even in the presence of birefringence, but noise dependent on axis needs to be studied further.

II. INTRODUCTION

Crystalline coatings (e.g. AlGaAs) have birefringence.

- `https://dcc.ligo.org/LIGO-G2200386`
- `https://www.nature.com/articles/nphoton.2013.174`
- `https://doi.org/10.1364/OPTICA.405938`

Polarization fluctuation and excess s-pol observed in LIGO.

- `https://dcc.ligo.org/LIGO-G2200559`

* yuta@caltech.edu

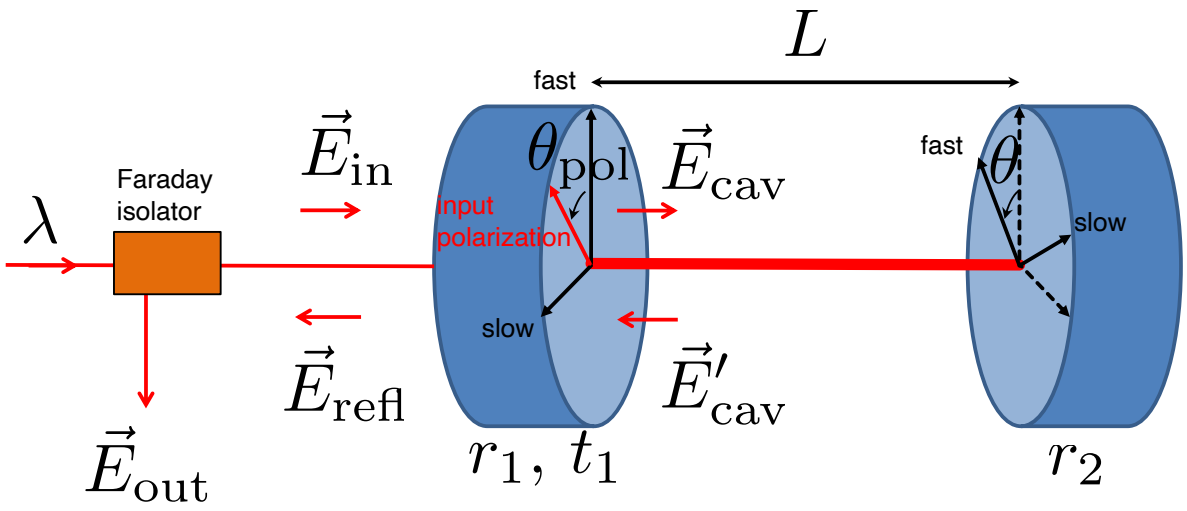

FIG. 1. Schematic of the Fabry-Perot cavity considered in this note. The fast axis of ETM is rotated by θ with respect to that of ITM.

- https://alog.ligo-la.caltech.edu/aLOG/index.php?callRep=60856
- https://dcc.ligo.org/DocDB/0183/G2201281/001/L1%20Commissioning%20Updated%20Aug%202022.pdf (last page; about 2% of s-pol from fully locked IFO; mostly from carrier higher order modes)

KAGRA is experiencing effects from sapphire ITM substrate birefringence.

- Birefringence observed in ITM single bounce, which can be explained by ITM substrate birefringence. https://gwdoc.icrr.u-tokyo.ac.jp/cgi-bin/DocDB/ShowDocument?docid=10369
- Sloshing observed in P-S coupled PRC. https://gwdoc.icrr.u-tokyo.ac.jp/cgi-bin/DocDB/ShowDocument?docid=10388
- Unwanted polarization reduces from "Lawrence effect" https://klog.icrr.u-tokyo.ac.jp/osl/?r=9393
- Polarization needs to be considered carefully when estimating cavity round-trip loss https://gwdoc.icrr.u-tokyo.ac.jp/cgi-bin/DocDB/ShowDocument?docid=11633

Experiments to detect vacuum magnetic birefringence (e.g. ALPS, PVLAS, OVAL) are suffering from birefringence noise. It is one of the limiting noise sources now.

- https://link.springer.com/article/10.1007/s00340-009-3677-7
- https://arxiv.org/abs/1710.03801
- https://link.springer.com/article/10.1140/epjc/s10052-018-6063-y
- https://www.sciencedirect.com/science/article/pii/S0370157320302428 (Full report of PVLAS. See Section 6.1 and 6.3)

III. THEORY

Schematic of the setup considered here is drawn in Fig. 1. The cavity length is L and the laser wavelength is λ. The fast axis of ETM coating is rotated by θ with respect to that of ITM. In the basis of ITM fast axis and slow axis,

the electric field of the input beam can be written as

$$\vec{E}_{\rm in} = \begin{pmatrix} \vec{e}_{\rm f} & \vec{e}_{\rm s} \end{pmatrix} \vec{v}_{\rm in} E_{\rm in}, \tag{1}$$

where $\vec{e}_{\rm f}$ and $\vec{e}_{\rm f}$ are eigen vectors along with ITM fast and slow axes, and $\vec{v}_{\rm in}$ is the vector representing the input polarization. The amplitude transmission of ITM can be written as

$$T_1 = \begin{pmatrix} t_1 e^{-i\Delta\phi_{t_1}} & 0 \\ 0 & t_1 \end{pmatrix}, \tag{2}$$

where $\Delta\phi_{t_1}$ is the phase difference between the fast and slow axes in ITM transmission, and t_1 is the amplitude transmission of ITM. Here, we assumed that the amplitude transmission is the same for both axes. We also assumed that substrate axis is the same as the coating axes[1]. Similarly, the amplitude reflectivity of ITM and ETM from HR side can be written as

$$R_{\rm i} = \begin{pmatrix} r_i e^{-i\Delta\phi_{r_i}} & 0 \\ 0 & r_i \end{pmatrix}, \tag{3}$$

where $\Delta\phi_{r_i}$ is the phase difference between the fast and slow axes in ITM/ETM transmission, and r_i is the amplitude transmission of ITM/ETM. $i = 1$ is for ITM and $i = 2$ is for ETM. Also, the amplitude reflectivity of ITM from AR side can be written as

$$S_1 = \begin{pmatrix} -r_1 e^{-i\Delta\phi_{s_1}} & 0 \\ 0 & -r_1 \end{pmatrix}, \tag{4}$$

where $\Delta\phi_{s_i}$ is the phase difference between the fast and slow axes in ITM reflection from AR side. Here, we use the convention that r_i and t_1 are real, and the sign is flipped for reflection from HR side and AR side. We keep the coordinate axis to be the same even if the propagation direction flips on mirror reflections, so that the sign for both polarizations will be the same.

A. Cavity eigenmodes

The electric field inside the cavity that propagates from ITM to ETM can be written as

$$\vec{E}_{\rm cav} = (I - A)^{-1} T_1 \vec{E}_{\rm in}, \tag{5}$$

with

$$A \equiv R_1 R(-\theta) R_2 R(\theta) e^{-i\phi}, \tag{6}$$

where $\phi = 4\pi L/\lambda$ is the phase acquired in the cavity round-trip and

$$R(\theta) \equiv \begin{pmatrix} \cos\theta & -\sin\theta \\ \sin\theta & \cos\theta \end{pmatrix}. \tag{7}$$

Note that ϕ includes phase acquired in the ITM and ETM reflection at slow axis. The resonant polarization mode is the eigenvectors of

$$M_{\rm cav} \equiv (I - A)^{-1} T_1. \tag{8}$$

Cavity enhancement factors for each mode will be the eigenvalues of $M_{\rm cav}$.

When $\theta = 0$, ITM axes and ETM axes are aligned, and the eigenvectors will be

$$\vec{v}_a = \begin{pmatrix} 1 \\ 0 \end{pmatrix}, \qquad \vec{v}_b = \begin{pmatrix} 0 \\ 1 \end{pmatrix}, \tag{9}$$

---

[1] We can generalize this later, if we want to consider the case when there are both coating and substrate birefringence

which means that resonant modes are linear polarizations along ITM fast axis $\vec{e}_f$ and slow axis $\vec{e}_s$. The cavity enhancement factors will be

$$w_a = \frac{t_1 e^{-i\Delta\phi_{t_1}}}{1 - r_1 r_2 e^{-i(\phi+\Delta\phi_{r_1}+\Delta\phi_{r_2})}}, \qquad w_b = \frac{t_1}{1 - r_1 r_2 e^{-i\phi}}. \tag{10}$$

The resonant frequency difference between two eigenmodes therefore will be

$$\Delta\nu = \frac{\Delta\phi_{r_1} + \Delta\phi_{r_2}}{2\pi}\nu_{\rm FSR}, \tag{11}$$

where $\nu_{\rm FSR} = c/(2L)$ is the free spectral range of the cavity.

When $\theta = \pi/2$, ITM fast axis and ETM slow axis are aligned, and the eigenvectors again will be

$$\vec{v}_a = \begin{pmatrix} 1 \\ 0 \end{pmatrix}, \qquad \vec{v}_b = \begin{pmatrix} 0 \\ 1 \end{pmatrix}. \tag{12}$$

The cavity enhancement factors will be

$$w_a = \frac{t_1 e^{-i\Delta\phi_{t_1}}}{1 - r_1 r_2 e^{-i(\phi+\Delta\phi_{r_1})}}, \qquad w_b = \frac{t_1}{1 - r_1 r_2 e^{-i(\phi+\Delta\phi_{r_2})}}. \tag{13}$$

The resonant frequency difference between two eigenmodes therefore will be

$$\Delta\nu = \frac{\Delta\phi_{r_1} - \Delta\phi_{r_2}}{2\pi}\nu_{\rm FSR}. \tag{14}$$

Since we defined the fast and slow axes so that $\Delta\phi_{r_i} > 0$, when $\theta = 0$, the resonant frequency difference is maximized, because the phase difference between slow and fast axes are added, and when $\theta = \pi/2$, it is minimized, because the phase difference is cancelled. In between $\theta = 0$ and $\theta = \pi/2$, the eigenmodes will no longer be liner polarizations, and the resonant frequency difference will be in between the maximum and the minimum.

When the resonant frequency difference is smaller than the cavity linewidth, $\Delta\phi_{r_i} \ll 2\pi/\mathcal{F}$, and when the effect from ITM substrate birefringence is small, $\Delta\phi_{t_1} \ll \Delta\phi_{r_1}\mathcal{F}/(2\pi)$, the resonant frequency difference can be calculated with

$$\Delta\nu \simeq \frac{2\pi(\arg w_1 - \arg w_2)}{\mathcal{F}}\frac{\nu_{\rm FSR}}{2\pi}, \tag{15}$$

at $\phi = 0$, where

$$\mathcal{F} = \frac{\pi\sqrt{r_1 r_2}}{1 - r_1 r_2} \tag{16}$$

is the finesse of the cavity. From Ref. [1], this can be approximated as

$$\Delta\nu \simeq \frac{\delta_{\rm EQ}}{2\pi}\nu_{\rm FSR} = \frac{\sqrt{(\Delta\phi_{r_1} - \Delta\phi_{r_2})^2 + 4\Delta\phi_{r_1}\Delta\phi_{r_2}\cos^2\theta}}{2\pi}\nu_{\rm FSR}, \tag{17}$$

for $\Delta\phi_{r_i} \ll 1$, and $\Delta\phi_{t_1} \ll \Delta\phi_{r_1}\mathcal{F}/(2\pi)$. Also, cavity eigenmodes can be approximated as

$$\vec{v}_a = \begin{pmatrix} \cos\theta_{\rm EQ} \\ \sin\theta_{\rm EQ} \end{pmatrix}, \qquad \vec{v}_b = \begin{pmatrix} -\sin\theta_{\rm EQ} \\ \cos\theta_{\rm EQ} \end{pmatrix}, \tag{18}$$

where

$$\cos 2\theta_{\rm EQ} = \frac{\dfrac{\Delta\phi'_{r_1}}{\Delta\phi_{r_2}} + \cos 2\theta}{\sqrt{\left(\dfrac{\Delta\phi'_{r_1}}{\Delta\phi_{r_2}} - 1\right)^2 + 4\dfrac{\Delta\phi'_{r_1}}{\Delta\phi_{r_2}}\cos^2\theta}}, \tag{19}$$

with

$$\Delta\phi'_{r_1} \equiv \Delta\phi_{r_1} + 2\pi\Delta\phi_{t_1}/\mathcal{F}. \tag{20}$$

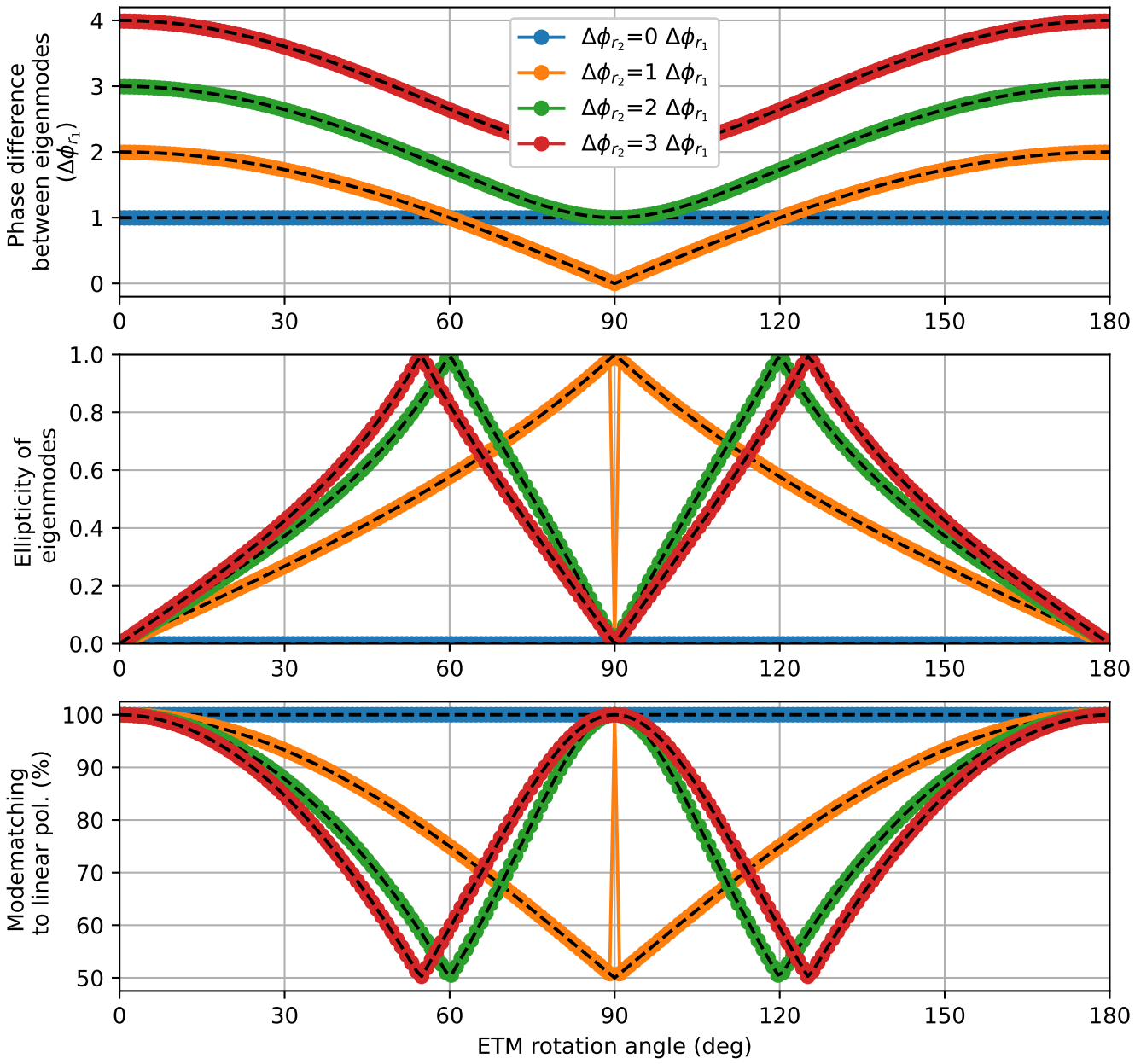

FIG. 2. Polarization eigenmodes of a Fabry-Perot cavity as a function of ETM rotation angle θ. The top panel shows the phase difference between eigenmodes in the unit of $\Delta\phi_{r_1}$. Black dashed lines are curves from Eq. (17) and Eq. (18). The middle panel shows the ellipticity of eigenmodes. The bottom panel shows the mode-matching ratio when the input beam polarization is aligned with ITM fast or slow axis.

The mode-matching ratio between the cavity polarization mode and the input beam can be calculated with

$$m = |\vec{v}_a \cdot \vec{v}_{\rm in}|^2. \tag{21}$$

Fig. 2 shows the result of numerical calculation for the phase difference between cavity eigenmodes, i.e. $2\pi\Delta\nu/\nu_{\rm FSR}$, (top), ellipticity of eigenmodes (middle), and the mode-matching ratio when the input beam polarization is linear and aligned with ITM fast or slow axis (bottom). In the calculation to generate these plots, we set $\Delta\phi_{t_1} = 0$. It is clear that the resonant frequency difference will be the maximum at $\theta = 0$, and minimized at $\theta = \pi/2$. In between, elliptic polarization will be cavity eigenmode. When $\theta = \pi/2$ and $\Delta\phi_{r_1} = \Delta\phi_{r_2}$, the phase difference between fast and slow axes is completely cancelled, and two modes will be degenerate. In this case, two linear polarizations will be

cavity eigenmodes, in other words, two circular polarizations will be cavity eigenmodes, since two modes have same resonant frequencies.

When the input polarization is linear and aligned with ITM axis, the mode-matching is maximized at $\theta = 0$ and $\theta = \pi/2$. In terms of maximizing the mode-matching and making resonant frequency difference large, aligning ETM rotation such that $\theta = 0$ and aligning the input polarization to ITM axis will be the optimal. **The requirement on the alignment will be not severe, i.e. within a few degrees or so, since the dependence on ETM rotation angle goes with θ^2 at $\theta = 0$.**

It is worth mentioning that cavity eigenmodes for the beam going in ITM to ETM and ETM to ITM are slightly different in general. The electric field inside the cavity that propagates from ETM to ITM can be written as

$$\vec{E}'_{\rm cav} = R(-\theta)R_2R(\theta)e^{-i\phi}M_{\rm cav}\vec{E}_{\rm in} \tag{22}$$

$$\equiv M'_{\rm cav}\vec{E}_{\rm in}. \tag{23}$$

Cavity eigenmodes in this direction will be eigenvectors of $M'_{\rm cav}$, and slightly different from those of $M_{\rm cav}$. When $\theta = 0$ or $\theta = \pi/2$, the eigenvectors will be the same with those of $M_{\rm cav}$,

$$\vec{v}'_a = \begin{pmatrix} 1 \\ 0 \end{pmatrix}, \qquad \vec{v}'_b = \begin{pmatrix} 0 \\ 1 \end{pmatrix}. \tag{24}$$

When $\theta = 0$, the cavity enhancement factors will be

$$w'_a = \frac{t_1 r_2 e^{-i(\phi+\Delta\phi_{t_1}+\Delta\phi_{r_2})}}{1 - r_1 r_2 e^{-i(\phi+\Delta\phi_{r_1}+\Delta\phi_{r_2})}}, \qquad w'_b = \frac{t_1 r_2 e^{-i\phi}}{1 - r_1 r_2 e^{-i\phi}}, \tag{25}$$

and when $\theta = \pi/2$, those will be

$$w'_a = \frac{t_1 r_2 e^{-i(\phi+\Delta\phi_{t_1})}}{1 - r_1 r_2 e^{-i(\phi+\Delta\phi_{r_1})}}, \qquad w'_b = \frac{t_1 r_2 e^{-i(\phi+\Delta\phi_{r_2})}}{1 - r_1 r_2 e^{-i(\phi+\Delta\phi_{r_2})}}. \tag{26}$$

Compared with w_a and w_b, those have extra phase ϕ from the cavity round trip and extra phase $\Delta\phi_{r_2}$ for corresponding axis for one additional reflection from ETM.

B. Cavity reflection

The electric field of the cavity reflection can be written as The electric field inside the cavity can be written as

$$\vec{E}_{\rm refl} = S_1\vec{E}_{\rm in} + T_1 M'_{\rm cav}\vec{E}_{\rm cav} \tag{27}$$

$$\equiv M_{\rm refl}\vec{E}_{\rm in} \tag{28}$$

where

$$M_{\rm refl} \equiv S_1 + T_1 M'_{\rm cav}. \tag{29}$$

The first term corresponds to the prompt reflection from ITM, and the second term is the ITM transmitted beam from cavity circulating beam. In general, when the input beam polarization component is

$$\vec{v}_{\rm in} = a\vec{v}'_a + b\vec{v}'_b, \tag{30}$$

the polarization component of the reflected beam is

$$M_{\rm refl}\vec{v}_{\rm in} = a(S_1 + w'_a T_1)\vec{v}'_a + b(S_1 + w'_b T_1)\vec{v}'_b. \tag{31}$$

Since the resonant condition of each eigenmode is generally different, it is generally not possible to make $|w'_a| = |w'_b|$. Therefore, the polarization component of the cavity reflected beam will be different from the input polarization.

When we use a Faraday isolator to extract the cavity reflection, we extract the polarization which is the same as the input polarization[2]. Therefore, the phase acquired from the cavity reflection can be calculated with

$$\arg(E_{\rm out}) = \arg(E_{\rm refl\parallel}) = \arg(M_{\rm refl}\vec{v}_{\rm in}\cdot\vec{v}_{\rm in}). \tag{32}$$

[2] It will be more complicated in gravitational wave detectors where input Faraday and output Faraday are not be perfectly aligned.

In the case when the input beam polarization is parallel to ITM fast axis, the reflected phase is the phase of (1,1) component of $M_{\rm refl}$, and that for ITM slow axis is (2,2) component of $M_{\rm refl}$.

To simplify, we first consider the case where the effects from ITM is dominant over those from ETM. If we set $\Delta\phi_{\rm r2} = 0$ and the input beam is linearly polarized with a polarization angle of $\theta_{\rm pol}$ such that

$$\vec{v}_{\rm in} = R(\theta_{\rm pol}) \begin{pmatrix} 1 \\ 0 \end{pmatrix} = \begin{pmatrix} \cos\theta_{\rm pol} \\ \sin\theta_{\rm pol} \end{pmatrix}, \tag{33}$$

Eq. (31) will be

$$M_{\rm refl}\vec{v}_{\rm in} = (S_1 + w'_a T_1) \begin{pmatrix} \cos\theta_{\rm pol} \\ 0 \end{pmatrix} + (S_1 + w'_b T_1) \begin{pmatrix} 0 \\ \sin\theta_{\rm pol} \end{pmatrix} \tag{34}$$

$$= \left(-r_1 e^{-i\Delta\phi_{s_1}} + \frac{t_1^2 r_2 e^{-i(\phi+2\Delta\phi_{t_1})}}{1 - r_1 r_2 e^{-i(\phi+\Delta\phi_{r_1})}} \right) \begin{pmatrix} \cos\theta_{\rm pol} \\ 0 \end{pmatrix} + \left(-r_1 + \frac{t_1^2 r_2 e^{-i\phi}}{1 - r_1 r_2 e^{-i\phi}} \right) \begin{pmatrix} 0 \\ \sin\theta_{\rm pol} \end{pmatrix}. \tag{35}$$

The reflected electric field in polarization parallel to $\vec{v}_{\rm in}$ and orthogonal polarization will be

$$E_{\rm refl\parallel} = M_{\rm refl}\vec{v}_{\rm in} \cdot \vec{v}_{\rm in} \tag{36}$$

$$= \left(-r_1 e^{-i\Delta\phi_{s_1}} + \frac{t_1^2 r_2 e^{-i(\phi+2\Delta\phi_{t_1})}}{1 - r_1 r_2 e^{-i(\phi+\Delta\phi_{r_1})}} \right) \cos^2\theta_{\rm pol} + \left(-r_1 + \frac{t_1^2 r_2 e^{-i\phi}}{1 - r_1 r_2 e^{-i\phi}} \right) \sin^2\theta_{\rm pol}, \tag{37}$$

$$E_{\rm refl\perp} = M_{\rm refl}\vec{v}_{\rm in} \cdot R(\theta_{\rm pol}) \begin{pmatrix} 0 \\ 1 \end{pmatrix} \tag{38}$$

$$= \left[-\left(-r_1 e^{-i\Delta\phi_{s_1}} + \frac{t_1^2 r_2 e^{-i(\phi+2\Delta\phi_{t_1})}}{1 - r_1 r_2 e^{-i(\phi+\Delta\phi_{r_1})}} \right) + \left(-r_1 + \frac{t_1^2 r_2 e^{-i\phi}}{1 - r_1 r_2 e^{-i\phi}} \right) \right] \cos\theta_{\rm pol} \sin\theta_{\rm pol}. \tag{39}$$

The case where ETM birefringence is dominant can be calculated by setting $\Delta\phi_{s_1} = \Delta\phi_{t_1} = 0$, and replacing $\Delta\phi_{\rm r_1}$ to $\Delta\phi_{\rm r_2}$ and $\theta_{\rm pol}$ to $\theta + \theta_{\rm pol}$.

When $\Delta\phi_{r_i} \ll 2\pi/\mathcal{F}$ and $r_2 = 1$ the phase of the reflected beam can be approximated as[3]

$$\arg\left(E_{\rm refl\parallel}\right) = (\Delta\phi_{\rm s_1} - 4\Delta\phi_{\rm t_1})\cos^2\theta_{\rm pol} - \frac{\mathcal{F}}{\pi}\left[\phi + \cos^2\theta_{\rm pol}\Delta\phi_{\rm r_1} + \cos^2(\theta + \theta_{\rm pol})\Delta\phi_{\rm r_2}\right] \tag{40}$$

The top two panels of Fig. 3 show the result of numerical calculation for the phase of the cavity reflected beam as a function of ETM rotation angle θ, when $\Delta\phi_{\rm t_1} = \Delta\phi_{\rm s_1} = 0$ and $\phi = 0$, for $\theta_{\rm pol} = 0$ and $\theta_{\rm pol} = \pi/2$. The bottom two panels show the same thing as a function of input beam polarization angle $\theta_{\rm pol}$ for $\theta = 0$ and $\theta = \pi/2$.

From the figure, it is clear that both ETM rotation angle and polarization angle changes the phase of the cavity reflected beam, and will contribute to the length noise, unless θ and $\theta_{\rm pol}$ are either 0 or $\pi/2$, where the effects are quadratic to the angles.

It is worth noting that, **even if we use this phase to lock the cavity, that does not mean that the cavity is locked to one of its polarization eigenmodes.**

Reflected phase in the orthogonal polarization can be calculated with

$$\arg\left(E_{\rm refl\perp}\right) = \arg\left(M_{\rm refl}\vec{v}_{\rm in} \cdot \vec{v}_{\rm in\perp}\right). \tag{41}$$

As we can see from Eq. (39), the orthogonal polarization is generated when two cavity eigenmodes are not co-resonant and $\theta_{\rm pol}$ is not 0 or $\pi/2$. It is generated from reflected electric field unbalance between two eigenmodes. Therefore, if $\Delta\phi_{r_i} \ll 2\pi/\mathcal{F}$, $\Delta\phi_{s_1} \ll 1$ and $\Delta\phi_{t_1} \ll 1$ is satisfied, the phase of $E_{\rm refl\perp}$ is always around $\pi/2$ away from the phase of $E_{\rm refl\parallel}$. This means that **the phase of the orthogonal polarization generated in the reflection is always around $\pi/2$ away, independent of the resonant condition of the cavity, whether the cavity is unlocked, locked on resonance or slightly detuned**. This means that, mode content of AS beam in the orthogonal polarization changes for FPMI, when the DARM offset is changed. Note that this does not mean that orthogonal polarization is off-resonant in recycling cavities, if there are any attached in the reflection. Phase inside the recycling cavity in orthogonal polarization will be shifted by $\pi/2$, but the resonant condition is determined only by its round-trip phase, not the initial phase [4].

---

[3] From numerical calculation. Can we show this? Note that $\Delta\phi_{\rm s_1}$ and $2\Delta\phi_{\rm t_1}$ do not cancel; only higher order content will cancel, as seen in the Lawrence effect, because higher order modes do not resonate in the cavity.

[4] In general, resonant condition of orthogonal polarization in power-recycling and signal-recycling could be different due to phase differences in BS reflection and transmission, and other birefringence effects.

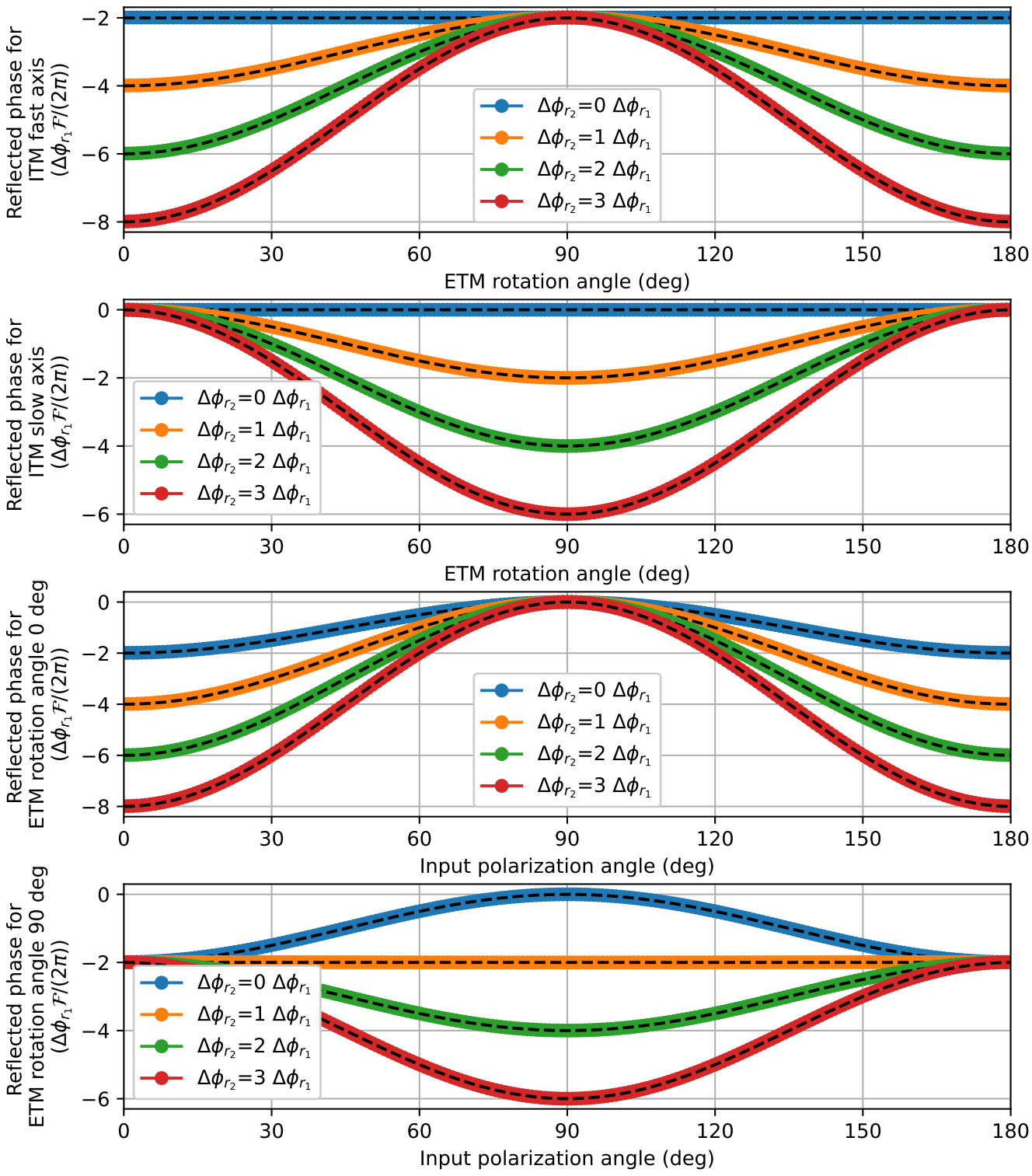

FIG. 3. The phase of the cavity reflected beam as a function of ETM rotation angle θ, when the input polarization is parallel to the ITM fast axis (panel 1) and slow axis (panel 2). The panel 3 and 4 show the phase of the cavity reflected beam as a function of input polarization angle $\theta_{\rm pol}$ when $\theta = 0$ deg and $\theta = 90$ deg. Black dashed lines are curves from Eq. (40).

IV. NOISE FROM COATING BIREFRINGENCE

In this section, we consider the case when the effect from coating birefringence is dominant over substrate birefringence. From Eq. (40), it is clear that $\Delta\phi_{\rm r1}$ and $\Delta\phi_{\rm r2}$ contributes more to the phase of the reflected beam, compared with $\Delta\phi_{\rm s1}$ and $\Delta\phi_{\rm t1}$, since the phase acquired inside the cavity is enhanced by a factor of $\mathcal{F}/(2\pi)$.

To clarify the effect from both fast axis and slow axis,we can decompose ϕ, $\Delta\phi_{\rm r1}$ and $\Delta\phi_{\rm r2}$ into phase acquired in the reflection in the both axes as

$$\phi = \phi_0 + \delta\phi_{\rm r_1 s} + \delta\phi_{\rm r_2 s} \tag{42}$$

$$\Delta\phi_{\rm r_i} = \delta\phi_{\rm r_i f} - \delta\phi_{\rm r_i s}. \tag{43}$$

With $\Delta\phi_{\rm s1} = \Delta\phi_{\rm t1} = 0$, Eq. (40) will be

$$\arg\left(E_{\rm out}\right) = -\frac{\mathcal{F}}{\pi}\left[\phi_0 + \cos^2\theta_{\rm pol}\delta\phi_{\rm r_1 f} + \sin^2\theta_{\rm pol}\delta\phi_{\rm r_1 s} + \cos^2\left(\theta+\theta_{\rm pol}\right)\delta\phi_{\rm r_2 f} + \sin^2\left(\theta+\theta_{\rm pol}\right)\delta\phi_{\rm r_2 s}\right]. \tag{44}$$

A. Noise from uniform static birefringence of coating

Even if the amount of phase acquire in the reflection for both axes $\delta\phi_{\rm r_i f/s}$ are constant, rotation of mirrors and input polarization creates noise. From Eq. (44), the phase noise from ETM rotation is

$$\frac{\delta L}{\delta\theta} = -\frac{\lambda}{2\pi}\sin\left[2(\theta+\theta_{\rm pol})\right]\Delta\phi_{\rm r_2}. \tag{45}$$

This is maximized when $\theta + \theta_{\rm pol} = \pi/4 + n\pi/2$ and will be

$$\frac{\delta L}{\delta\theta} = -\frac{\lambda}{2\pi}\Delta\phi_{\rm r_2}. \tag{46}$$

Similarly from Eq. (44),

$$\frac{\delta L}{\delta\theta_{\rm pol}} = -\frac{\lambda}{2\pi}\left[\sin 2\theta_{\rm pol}\Delta\phi_{\rm r_1} + \sin\left[2(\theta+\theta_{\rm pol})\right]\Delta\phi_{\rm r_2}\right]. \tag{47}$$

This is maximized when $\theta = \pi/4 + n\pi/2$ and $\theta + \theta_{\rm pol} = \pi/4 + m\pi/2$,

$$\frac{\delta L}{\delta\theta_{\rm pol}} = -\frac{\lambda}{2\pi}(\Delta\phi_{\rm r1} + \Delta\phi_{\rm r2}). \tag{48}$$

Let us consider the length noise from static birefringence of AlGaAs coating for various laser interferometric gravitational wave detectors. Various experiments measured the resonant frequency split in linear cavities, and using Eq. (11) or Eq. (14), $\Delta\phi_{\rm r1}$ and $\Delta\phi_{\rm r2}$ can be estimated. Below is the summary of the literature.

- Syracuse group [2] measured $\Delta\nu = 500$ kHz in $\nu_{\rm FSR} = 1.5$ GHz cavity, indicating $\Delta\phi_{\rm r1} \pm \Delta\phi_{\rm r2} \sim 2\times10^{-3}$ rad.
- Caltech group [3] measured $\Delta\nu = 1.4$ MHz in $\nu_{\rm FSR} = 4$ GHz cavity, indicating $\Delta\phi_{\rm r1} \pm \Delta\phi_{\rm r2} \sim 2\times10^{-3}$ rad.
- Ref. [4] repoted $\Delta\nu = 110$ kHz in $\nu_{\rm FSR} = 490$ MHz cavity, indicating $\Delta\phi_{\rm r1} \pm \Delta\phi_{\rm r2} \sim 1\times10^{-3}$ rad.
- Ref. [5] repoted $\Delta\nu = 4$ MHz in $\nu_{\rm FSR} = 4.3$ GHz cavity, indicating $\Delta\phi_{\rm r1} \pm \Delta\phi_{\rm r2} \sim 6\times10^{-3}$ rad.

Fig. 4 show the estimated displacement noise from ETM rotation and input polarization rotation, using Eq. (46) and Eq. (48) as a worst case scenario, and $\Delta\phi_{\rm r1} = \Delta\phi_{\rm r2} = 1\times10^{-3}$ rad. Since Eq. (46) and Eq. (48) only differ by a factor of 2 in this case, only Eq. (48) is plotted. For simplicity, $\lambda = 1064$ nm is used, although some interferometers use different wavelength. From the figure, it is clear that AlGaAs coating birefringence will not be a limiting noise for gravitational wave detectors when $\delta\theta$ and $\delta\theta_{\rm pol}$ are in the order of $1\times(1\ {\rm Hz}/f^2)$ nrad$/\sqrt{\rm Hz}$.

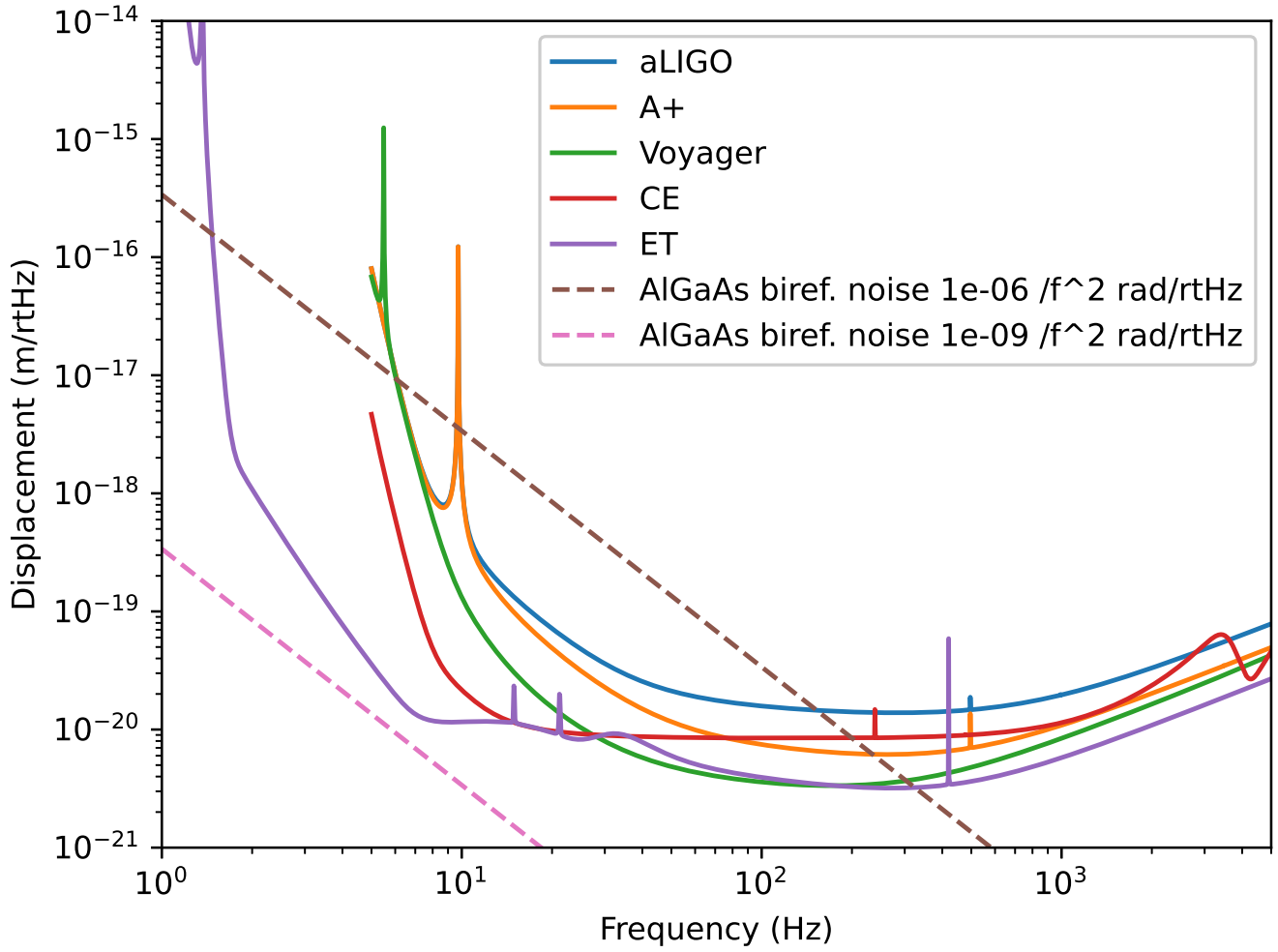

FIG. 4. Estimated displacement noise from mirror or input beam polarization rotation coupled to AlGaAs coating birefringence in the worst case scenario with $\Delta\phi_{\rm r1} = \Delta\phi_{\rm r2} = 1 \times 10^{-3}$ rad (dashed lines), compared with designed displacement sensitivity of various gravitational wave detectors (solid lines). Two cases where $\delta\theta$ or $\delta\theta_{\rm pol}$ is $1{\times}(1\ {\rm Hz}/f^2)$ $\mu{\rm rad}/\sqrt{\rm Hz}$ and $1{\times}(1\ {\rm Hz}/f^2)$ ${\rm nrad}/\sqrt{\rm Hz}$ are plotted.

B. Noise from fluctuations of coating birefringence

When the refractive index of the coating fluctuates in the fast axis and the slow axis, it will create fluctuating $\delta\phi_{\rm r_if/s}$. From Eq. (44), when the amount of fluctuations in $\delta\phi_{\rm r_if/s}$ are equivalent and incoherent, the total noise from these fluctuations will be the same for all θ and $\theta_{\rm pol}$. However, **if there are anti-correlations in $\delta\phi_{\rm r_if}$ and $\delta\phi_{\rm r_is}$, there are certain θ that cancels noise from ITM and $\theta + \theta_{\rm pol}$ that cancels noise from ETM.** Such anti-correlation was recently reported in Ref. [6]. When $\delta\phi_{\rm r_1f} = -\delta\phi_{\rm r_1s}$ and $\delta\phi_{\rm r_2f} = -\delta\phi_{\rm r_2s}$, the cancellation is obtained when $\theta_{\rm pol} = \pi/4$ and $\theta = 0$ or $\theta = \pi/2$.

V. POWER LOSSES FROM BIREFRINGENCE

In this section, we discuss power and mode content of cavity reflected beam. To simplify, we first consider the the case where the effects from ITM is dominant over those from ETM, as we considered in Eq. (37) and Eq. (39). When

the cavity is not resonant, the power loss to orthogonal polarization will be

$$P_{\mathrm{refl}\perp} = |E_{\mathrm{refl}\perp}|^2 = |r_1^2(1-e^{-i\Delta\phi_{s_1}})\cos\theta_{\mathrm{pol}}\sin\theta_{\mathrm{pol}}|^2 \tag{49}$$

$$\simeq r_1^2(\Delta\phi_{s_1})^2\cos^2\theta_{\mathrm{pol}}\sin^2\theta_{\mathrm{pol}}, \tag{50}$$

for $\Delta\phi_{s_1} \ll 1$. When the cavity is locked to TEM00 mode using a reflected phase in Eq. (40), $\phi + \cos^2\theta_{\mathrm{pol}}\Delta\phi_{r_1} \simeq 2\pi n$ is satisfied. In this case, with $\Delta\phi_{r_1} \ll 2\pi/\mathcal{F}$, the power loss to orthogonal polarization will be

$$P_{\mathrm{refl}\perp} \simeq \left|\left[-\left(-r_1e^{-i\Delta\phi_{s_1}} + \frac{t_1^2r_2}{1-r_1r_2}e^{-i(2\Delta\phi_{t_1}+\frac{\mathcal{F}}{2\pi}\sin^2\theta_{\mathrm{pol}}\Delta\phi_{r_1})}\right) + \left(-r_1 + \frac{t_1^2r_2}{1-r_1r_2}e^{+i\frac{\mathcal{F}}{2\pi}\cos^2\theta_{\mathrm{pol}}\Delta\phi_{r_1}}\right)\right]\cos\theta_{\mathrm{pol}}\sin\theta_{\mathrm{pol}}\right|^2. \tag{51}$$

For $r_2 = 1$, $r_1 \simeq 1$, $t_1^2 = 1 - r_1^2$, $\Delta\phi_{t_1} \ll 1$ and $\Delta\phi_{s_1} \ll 1$, this reduces to

$$P_{\mathrm{refl}\perp} \simeq \left|\left[-\left(-r_1e^{-i\Delta\phi_{s_1}} + (1+r_1)e^{-i(2\Delta\phi_{t_1}+\frac{\mathcal{F}}{2\pi}\sin^2\theta_{\mathrm{pol}}\Delta\phi_{r_1})}\right) + \left(-r_1 + (1+r_1)e^{+i\frac{\mathcal{F}}{2\pi}\cos^2\theta_{\mathrm{pol}}\Delta\phi_{r_1}}\right)\right]\cos\theta_{\mathrm{pol}}\sin\theta_{\mathrm{pol}}\right|^2 \tag{52}$$

$$\simeq \left|i\left(-r_1\Delta\phi_{s_1} + 2(1+r_1)\Delta\phi_{t_1} + \frac{\mathcal{F}}{2\pi}(1+r_1)\Delta\phi_{r_1}\right)\right|^2\cos^2\theta_{\mathrm{pol}}\sin^2\theta_{\mathrm{pol}} \tag{53}$$

$$\simeq \left(\Delta\phi_{s_1} - 4\Delta\phi_{t_1} - \frac{\mathcal{F}}{\pi}\Delta\phi_{r_1}\right)^2\cos^2\theta_{\mathrm{pol}}\sin^2\theta_{\mathrm{pol}}. \tag{54}$$

The first term comes from the polarization rotation in the prompt reflection from ITM, and the second term comes from the polarization rotation in the transmission of ITM, which happens twice. The third term comes from detuning of the cavity from its polarization eigenmodes.

So far, we have considered uniform birefringence over the mirror. For perturbation from the uniform birefringence, higer order modes are generated. When the cavity is not resonant, the amount of higher order modes in orthogonal polarization will be

$$P_{\mathrm{refl}\perp}^{\mathrm{HOM}} \simeq r_1^2(\Delta\phi_{s_1}^{\mathrm{HOM}})^2\cos^2\theta_{\mathrm{pol}}\sin^2\theta_{\mathrm{pol}}. \tag{55}$$

The amount when the cavity is locked will be

$$P_{\mathrm{refl}\perp}^{\mathrm{HOM}} \simeq \left(\Delta\phi_{s_1}^{\mathrm{HOM}} - 2\Delta\phi_{t_1}^{\mathrm{HOM}}\right)^2\cos^2\theta_{\mathrm{pol}}\sin^2\theta_{\mathrm{pol}}. \tag{56}$$

Note that, coefficient of $\Delta\phi_{t_1}^{\mathrm{HOM}}$ is 2, as opposed to 4 for $\Delta\phi_{t_1}$ in Eq. (54), since higher order modes do not resonate in the cavity and higher order modes are generated in the ITM transmission of intra-cavity beam, which happens once.

A. ITM substrate birefringence

When the effect from ITM substrate birefringence dominates, we can set $\Delta\phi_{r_1} = 0$. Also, $\Delta\phi_{s_1} = 2\Delta\phi_{t_1}$ and $\Delta\phi_{s_1}^{\mathrm{HOM}} = 2\Delta\phi_{t_1}^{\mathrm{HOM}}$, as ITM back reflection passes through ITM substrate twice. In this case, amount of TEM00 orthogonal polarization stays the same when the cavity is locked or unlocked, as apparent from Eq. (50) and Eq. (54). As for higher order modes, the amount is suppressed to the second order effect when the cavity is locked. This is similar to Lawrence effect for ITM thermal lensing [7], and was observed in KAGRA, which have non-uniform birefringence from sapphire ITM [8, 9].

B. ITM coating birefringence

When the effect from ITM coating birefringence dominates, we can set $\Delta\phi_{s_1} = \Delta\phi_{r_1}$[5]. $\Delta\phi_{s_1}$ is not exactly $2\Delta\phi_{t_1}$, as penetration length for coating is different from coating thickness. Therefore, **Lawrence effect does not completely suppress the higher order modes.** If we can set $\Delta\phi_{s_1} = 2l\Delta\phi_{t_1}$, where $l < 1$ is the ratio of the penetration length over coating thickness, higher order mode in orthogonal polarization increases when the cavity is locked, for $l < 0.5$ (see Table I). TEM00 mode in orthogonal polarization increases, as $\mathcal{F}/\pi \gg 1$.

See, also Ref. [10] for possible explanations of excess s-polarization measured at LLO.

---

[5] There could be a possibility that birefringence is not uniform over coating thickness. For example, birefringence might be larger at mirror-coating boundary from stresses. Qualitative explanation remains the same also in such cases.

TABLE I. Change in the power of light in orthogonal polarization when the cavity is unlocked to locked for different modes. The cases when the effect from different birefringence dominates are shown. A common factor $\cos^2(\theta+\theta_{\rm pol})\sin^2(\theta+\theta_{\rm pol})$ is omitted.

	ITM substrate	ITM coating	ETM coating
Carrier TEM00	$(2\Delta\phi_{t_1})^2$ to $(2\Delta\phi_{t_1})^2$	$(\Delta\phi_{r_1})^2$ to $(1-2/l-\mathcal{F}/\pi)^2(\Delta\phi_{r_1})^2$	0 to $(\mathcal{F}/\pi\times\Delta\phi_{r_2})^2$
	(same)	(increase)	(increase)
Carrier HOM	$(2\Delta\phi_{\rm t_1}^{\rm HOM})^2$ to $O((\Delta\phi_{\rm t_1}^{\rm HOM})^4)$	$(\Delta\phi_{r_1}^{\rm HOM})^2$ to $(1-1/l)^2(\Delta\phi_{r_1}^{\rm HOM})^2$	0 to 0
	(reduce)	(remains)	(none)
RF sidebands	$(2\Delta\phi_{t_1})^2$ to $(2\Delta\phi_{t_1})^2$	$(\Delta\phi_{r_1})^2$ to $(\Delta\phi_{r_1})^2$	0 to 0
	(same)	(same)	(none)

C. ETM coating birefringence

Let us next consider the case when the effect from ITM substrate/coating birefringence is negligible compared with ETM. In this case, we can set $\Delta\phi_{\rm s_1}=\Delta\phi_{\rm t_1}=\Delta\phi_{\rm r_1}=0$. The power loss to orthogonal polarization when the cavity is unlocked will be zero, and that when the cavity is locked can be obtained by replacing $\Delta\phi_{\rm r_1}$ to $\Delta\phi_{\rm r_2}$ and $\theta_{\rm pol}$ to $\theta+\theta_{\rm pol}$ in Eq. (54),

$$P_{\rm refl\perp}\simeq\left(\frac{\mathcal{F}}{\pi}\Delta\phi_{r_2}\right)^2\cos^2(\theta+\theta_{\rm pol})\sin^2(\theta+\theta_{\rm pol}). \tag{57}$$

In this case, the power loss increases when the cavity is locked, and the mode content will be only carrier TEM00 mode.

[1] F. Brandi *et al.*, Appl. Phys. B **65**, 351–355 (1997).
[2] S. Tanioka, *Current status of AlGaAs electro-optic effect measurement*, LIGO-G2200386 .
[3] Tara Chalermsongsak Evan Hall, *Inserting AlGaAs cavities*, `https://nodus.ligo.caltech.edu:8081/CTN/1474` (2014).
[4] G. Winkler *et al.*, Optica **8**, 686 (2021).
[5] G. D. Cole *et al.*, Nature Photonics **7**, 644 (2013).
[6] J. Yu *et al.*, *Noise contributions in crystalline mirror coatings*, 2022 Joint conference of the European Frequency and Time Forum the IEEE International Frequency Control Symposium, April 24-28 (2022).
[7] R. C. Lawrence, *Active wavefront correction in laser interferometric gravitational wave detectors*, MIT Ph.D. Thesis (2003).
[8] Y. Michimura *et al.*, *P-pol from ITMX is smaller by a factor of 3 with Xarm locked*, `https://klog.icrr.u-tokyo.ac.jp/osl/?r=9393` (2019).
[9] Y. Michimura *et al.*, *Arm cavity round-trip loss measurement with ITM inhomogeneity and birefringence*, JGW-T201163.
[10] Y. Michimura, M. Nakano, *Note on power measured at OFI s-pol rejected light monitor*, LIGO-G2201296.